MULTI-PSF MODELLING FOR X-RAY DIFFRACTION PATTERN RECONSTRUCTION

Daan Zhu, Moe Razaz, Andrew Hemmnings and Binhai Wang

School of Computing Sciences, University of East Anglia
Norwich NR4 7TJ, England
d.zhu@uea.ac.uk

ABSTRACT

In this paper, we present a point spread function (PSF) modelling technique to improve restoration of x-ray diffraction pattern (XRD). Different diffraction areas have different distortion orientations due to diffuse light distortion (DLD). A new multiple PSF model is introduced and used to restore XRD data. Raw PSFs are collected from isolated spots from x-ray diffraction pattern in high resolution areas which represent orientation of DLDs. An adaptive ridge regression (ARR) technique is used to remove noise from the raw PSF. A target Gaussian function is used to model the raw PSFs. A gradient descent algorithm (GDA) is used to find optimum parameters in a Gaussian function. A set of XRD data are restored by an iterative deconvolution algorithm (IDA) using the modelled PSFs. Experimental results using a single and multiple PSFs are presented and discussed. We show that by using a multiple PSF model in the deconvolution algorithm improved restored X-ray patterns are obtained and as a result the symmetry estimator and χ^2 are improved.

1. INTRODUCTION

X-ray diffraction analysis and nuclear magnetic resonance (NMR) are crucial techniques in macromolecule structure determination [1]. Each diffraction peak corresponds to a point in the reciprocal lattice and represents a wave with an amplitude and a relative phase. However, x-ray diffraction data are degraded when it passes through an x-ray diffraction system. The PSF of an imaging system provides a complete, quantitative description of this resolution and directly characterizes the image degradation within the system. Implementation of deconvolution techniques on x-ray diffraction pattern dates back to Rafaja's work in [2]. Rafaja employed a stoke deconvolution algorithm to restore 1D diffraction data. The degradation model is assumed to have Gaussian smoothing, which is commonly found in most optical microscopy. From the literature review, so far there are few publications on PSF measurement in x-ray diffraction systems. Dougherty [3] et. al. measured PSF by using a pinhole. However, in practice the pinhole is not infinitely small and the image obtained will be an image of the focal spot blurred and the assumption of this blurred model is based on the radially-symmetric Gaussian model.

X-ray system function, namely PSF determination, is difficult in reconstruction of XRD data. Unfortunately, direct or indirect methods which have successfully been used to measure PSFs of microscopy systems are difficult to use on x-ray diffraction systems. Quabis [5] summarized experimental and theoretical methods to measure PSFs of tomography microscopy. Lehr [6] use another two indirectly or directly measure PSFs of x-ray microscopy. The PSFs obtained from experiments should consist of diffraction rings that grow symmetrically on either side of focus.

Razaz et al [8, 9] developed a novel method to model and measure PSF from 1D NMR data, which was successfully applied to 1D and 2D NMR deconvolution. An isolated peak is selected from the original 1D NMR data. This idea can be extended to PSF measurement of an x-ray diffraction system. Generally, isolated peaks in high resolution data near the edge of XRD system are distorted by DLD. In this paper, the modelled PSFs from isolated peaks are used for restoration of real XRD data. The algorithm we used is the iterative deconvolution algorithm (IDA) presented in [7].

2. SYSTEM DISTORTION

Degradation is mainly caused by diffracted light. An example is shown here Fig. (1). The diffraction pattern in Fig. (1) is a quarter of a whole diffraction pattern. A area which is presented in Fig. (1) is selected from the upper left corner from a full XRD data. It is normally assumed that a diffraction spot is a circle, when it passes through an x-ray diffraction system. However the DLD causes the diffraction spot become to an ellipse. Far away from the central x-ray pattern, more serious distortions are caused. Such distortion makes x-ray analysis difficult [10]. The distorted diffraction peaks cause their change of diffraction intensity and change of width, length and shape of diffraction spots. The degraded diffraction spots cause problem in crystal structure analysis, such as phase identification, line profile analysis of microstructure [10]. Two different pattern can be extracted from high resolution XRD data. Figure (2 a) shows a real zoom-in extracted pattern from the upper-left corner of the XRD data and Fig. (2 b) shows an extracted pattern from the upper-right corner. As can be seen the orientation of spots in the two pictures are different. The full size of this test XRD image is 2048×2048 pixels.

3. PROBLEM FORMULATION

Several isolated spots are selected from the XRD which are used to develop our multiple PSF deconvolution algorithm.

3.1 Multi-PSF modelling

To develop a multi-PSF model, a full XRD data is equally divided into four or nine areas which correspond to different distortion orientations. An isolated spot which presents the local DLD, is selected from different diffraction data. This isolated spot is used as a raw PSF data. Figure 4 shows DLD orientations in a typical XRD data. The shape and orientation

ORS and School of Computing Science Funding this work

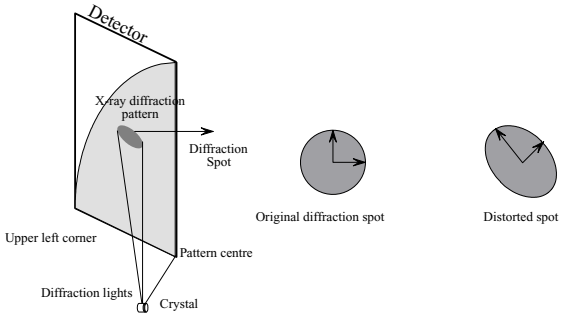

Figure 1: Diffuse light distortion

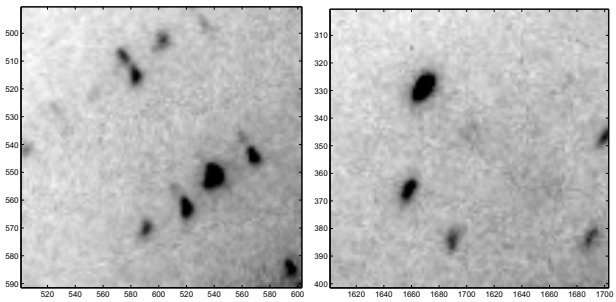

(a) Upper-left corner of an XRD data (b) Upper-right corner of an XRD data

Figure 2: Corner extracted pattern

of one, four and nine PSFs are shown. The assumed isolated is a 2D Gaussian. The standard derivation of Gaussian along x and y axes are unknow. In the next step, a set of algorithms will be used to specify the size of PSF from modelling a raw isolated peak. Figure (3) summarizes the modelling process for a PSF of an XRD imaging system.

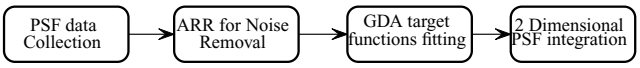

Figure 3: Block diagram representing PSF modelling

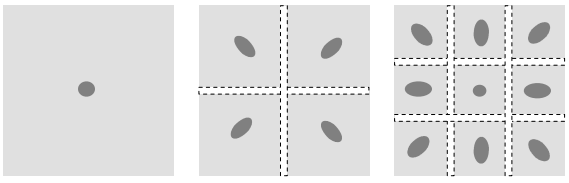

(a) One PSF (b) Four PSFs (c) Nine PSFs

Figure 4: PSFs orientation in different areas

3.2 ARR Noise removal

A raw PSF is noisy. Figure (5) shows an intensity of an XRD.

Direct use of raw PSF for restoration leads to poor restored results [7]. We need to remove noise and reset the baseline. We use an adaptive ridge regression (ARR), a special form of ridge regression, balancing the quadratic penal-

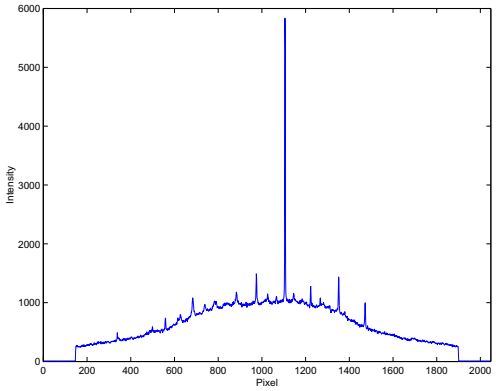

Figure 5: Intensity of an XRD

ization on each parameter of the model [12]. The mathematical expression is shown below

$$\hat{w} = min\{\sum_{i=1}^{N}(\sum_{j=1}^{N}(w_j\Phi_{ij}(x) - \hat{y}_i)^2 + \lambda\sum_{j=1}^{N}w_j^2)\} \qquad (1)$$

where λ is the Lagrange multiplier, which can be a vector or a scalar. To avoid the simultaneous estimation of the N hyper-parameters by trial [12], a constraint equation is introduced

$$\frac{1}{N}\sum_{j=1}^{N}\frac{1}{\lambda_j} = \frac{1}{\lambda} \qquad (2)$$

Minimization of equation (1) provides an optimized w. The choice of λ is important. If λ is small, the coefficients with small mean least square (MLS) estimate are heavily penalized. In this case, it has a good performance in fitting, but it can not remove noise well. To solve equation (1) we introduce two new parameters

$$r_j = \sqrt{\frac{\lambda_j}{\lambda}}w_j \quad ; \qquad j = 1,2,\cdots,N \qquad (3)$$

and

$$c_j = \sqrt{\frac{\lambda}{\lambda_j}} \quad ; \qquad j = 1,2,\cdots,N \qquad (4)$$

r_j and c_j can be derived using a similar produce as in [11, 12]. The optimization of equation (1) subject to constraint equation in (2) leads to

$$\begin{cases} \{\sum_{i=1}^{N}(\sum_{j=1}^{N}(c_j r_j\Phi_{ij}(x) - \hat{y}_i)^2 + \lambda\sum_{j=1}^{N}r_j^2)\}_{min} \\ s.t. \qquad \sum_{j=1}^{N}c_j^2 = N, c_j \geq 0 \end{cases} \qquad (5)$$

Grandvalet [12] uses expectation maximization (EM) to find an optimized solution. The EM derivation for calculation of c_j and r are presented below

$$c_j^{(k+1)} = \frac{N r_j^{(k)^2}}{\sum_{k=1}^{N} r_k^{(k)^2}} \qquad (6)$$

$$r^{(k+1)} = \frac{diag(\mathbf{c}^{(k+1)}) \cdot \Phi(x)^T \mathbf{y}}{diag(\mathbf{c}^{(k+1)}) \cdot \Phi(x)^T \Phi(x) \cdot diag(\mathbf{c}^{(k+1)}) + \lambda I} \quad (7)$$

where I is an identity matrix, and $diag(c)$ is a diagonal matrix. The sufficient condition for existence of inverse root of equation (7) is that λ must not be zero.

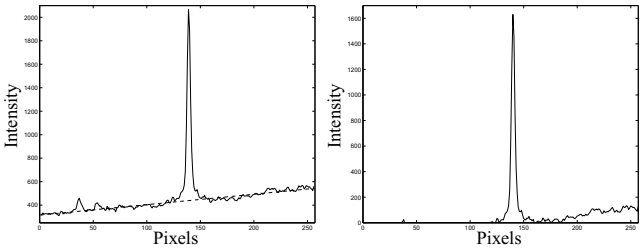

(a) Raw PSF (b) Modelled PSF with λ=0.03

Figure 6: Raw PSF and ARR modelled PSF

3.3 GDA optimization

The filtered raw isolated peak through ARR still includes noise. A gradient descent algorithm (GDA) is employed to model filtered PSF by using a Gaussian function. The problem can be formalized by minimizing the summed square error between target and raw functions as

$$E = \sum_{n=1}^{N} (y(n) - \hat{y}(n))^2 \quad (8)$$

Then we have

$$E(\delta) = \sum_{i=1}^{N} [e^{-\frac{x_i^2}{2\sigma^2}} - f(x_i)]^2 \quad (9)$$

where σ is the Gaussian parameter and E denotes an error function. The corresponding column vector $\hat{\mathbf{y}} = \mathbf{XT}$ where $\mathbf{T}$ is a weighting vector. By using first derivative of E with respect to $\mathbf{T}$ zero, we have

$$\frac{\partial E}{\partial \mathbf{T}} = 2\mathbf{X}^T\mathbf{XT} - 2\mathbf{X}^T\mathbf{y} = 0 \quad (10)$$

or

$$\mathbf{T} = (\mathbf{X}^T\mathbf{X})^{-1}\mathbf{X}^T\mathbf{y} \quad (11)$$

The expression $(\mathbf{X}^T\mathbf{X})^{-1}\mathbf{X}^T$ is the *pseudoinverse* of matrix $\mathbf{X}$. If matrix $\mathbf{X}$ is not quadratic, the normal inverse does not exist and therefore there are no optimum solution can be found. A simplified version of the GDA is shown below:

1 *Initialize* $\mathbf{T} = t_0$
2 *Test* $t_1 = t_0 + \Delta t$. *In the first iteration set* $\Delta t = 1$
3 *If* $\frac{dE}{dt_1} > 0$ *Then* $t_1 = -t_1$; *If* $-\frac{dE}{dt_1} > 0$ *Then decrease* Δt *and repeat* 2
4 $t_{i+1} = t_i + \alpha \frac{dE}{dt_i}$
5 *If* $E_{i+1} > E_i$ *or* $\frac{dE}{d(t_{i+1})} < \varepsilon$; *Then stop and go to end*
If $E_{i+1} > E_i$ *and* $\frac{dE}{d(t_{i+1})} > \varepsilon$; *change* α *repeat from* 3
6 *End*

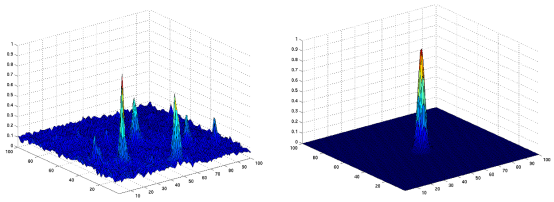

(a) A raw peak (b) Modelled PSF

Figure 7: Raw PSF and modelled PSF

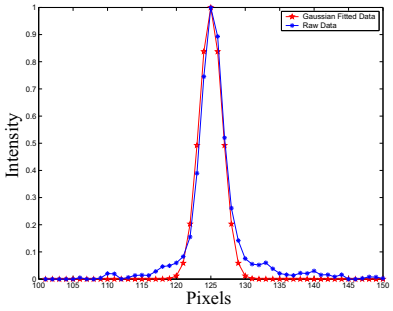

Figure 8: GDA fitted PSF in 1D plots

The parameter α can be adjusted to change the rate of convergence of the algorithm. Figure (7) shows raw peaks and a modelled PSF.

The same method is employed to model the isolated peaks selected from different XRD. The deconvolution algorithm IDA [7] is used for restoration of degraded XRD data.

4. EXPERIMENTAL RESULTS

Some experimental results will be presented in this section. The x-ray diffraction instrument we used is Rigaku R-axis IV with a Mar CCD detector. A post-processing software is *Denzo* [13] for integration of x-ray diffraction data to calculate the electronic density map. The test crystal is the sperm myoglobin H64Y mutant. The symmetry of the test crystal is primitive hexagonal *P6*. Figure (9) compares the XRD integration pattern. The red peaks are the wrong peaks against symmetry. Table 1 compares the original and restored XRD data. The data restoration has been achieved using single PSF and multiple-PSF models. It can be seen that the restored data using a single-PSF model has a reduced Distortion Index than the raw XRD data. The use of multiple PSF models has lead to smaller values for the Distortion Index and integration error χ^2.

Table 1: Comparison pattern analysis

Diffraction Pattern	Original pattern	One PSF restoration	Four PSFs restoration	Nine PSFs restoration
Selected spots	1527	1935	1844	1779
Rejected spots	96	208	71	105
Accepted rate	93.71%	89.25%	96.14%	94.09%
χ^2 x-direction	2.60	3.19	2.81	1.99
χ^2 y-direction	1.87	2.61	2.52	2.02
Distortion Index	0.67%	0.07%	0.04%	0.04%

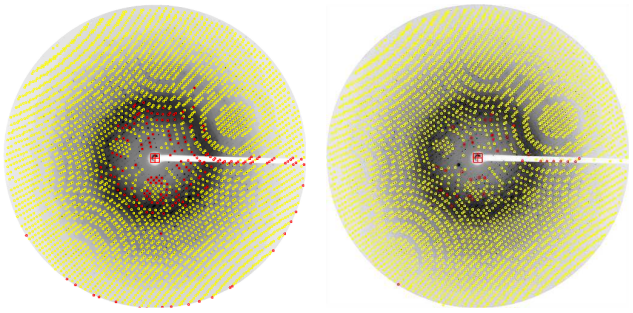

(a) Original integration pattern (b) Restored integration pattern with 9 PSFs based model

Figure 9: Comparison of integration patterns

5. CONCLUSION

In this paper, we select isolated spots from different areas of a XRD image. ARR and GDA are first used to model raw PSF and remove noise. Due to DLD, the diffraction spots cause distortion especially the diffraction spots in high resolution areas. Because different areas on an XRD image have different orientations, we developed a multi-PSF scheme to restore XRD data. We have found that restored and original XRD are compared and analyzed. The symmetry estimator is improved and the integration error χ^2 are often decreased after restoration.

REFERENCES

[1] R.C. Charles and R.S. Taul, "Biophysical Chemistry Part 2 Techniques for the study of Biological structure and faction", *W.H.Freeman and Company New York*, 1980

[2] D. Rafaja, "Deconvolution versus convolution-a comparison for materials with concentration gradient", *Materials Structure*, vol. 7, pp. 43-50, 2000

[3] G. Dougherty and Z.Kawaf, "The point spread function revisited: image restoration using 2-D deconvolution", *Radiography*, vol. 7, pp. 255-262, 2001

[4] M. Pokrić and N.M. Allinson, "Testing of gadolinium oxy-sulphide phosohors for use in CCD-based X-ray detectors for macromolecular crystallography", *Nuclear Instruments and Methods in Physics Research A*, vol. 477, pp. "353-359, 2002

[5] S.Quabis, R.Dorn, M.Eberler and Q.Glockl and G.Leuchs,"The focus of light-theoretical calculation and experimental tomographic reconstruction", *Applied physics B Lasers and Optics*, vol. B72, pp. 109-113, 2001

[6] J. Lehr, B.J. Sibarita and M.J.Chassery, "Image restoration in x-ray microscopy: PSF determination and biological application", *IEEE transaction on image processing*, vol. 7, pp. 258-263, 1998

[7] M. Razaz and R.Lee, "Comparison of an iterative deconvoltion and Wiener Filter for image restoration", *Image Processing Mathematics and Application*, Oxford University Press, pp. 145-159, 1997

[8] M. Razaz, R. A. Lee, P. S. Belton and K. M. Wright, "A new approach for restoration of NMR signals", *Signal processing IX, Theories and Application*, Vol. 2 pp. 841-844, 1998

[9] M. Razaz, R. A. Lee, P. S. Belton and K. M. Wright", "A new algorithm for deconvolution of NMR spectra and images", *Image Processing, Mathematical Methods and Application*, vol. 2, pp. 94-114, 2000

[10] D. Louër and E.J.Mittemeijer, "Materials Science Forum", "Chapter: Proceedings of the 7th European Powder Diffraction Conference", vol. 378-381, *Science and Engineering Press*, 2001

[11] M.E.Tipping, "Spare Bayesian Learning and the Relevance Vector Machine", *Journal of Machine learning Research*, vol. 1, pp. 211-244, 2001

[12] Y.Grandvalet, "Least absolute shrinkage is equivalent to quadratic penalization", *International Conference on Artificial Neural Networks*, 1998

[13] Z. Otwinowski and W. Minor, "Macromolecular Crystallography, part A", "Chapter Processing of X-ray Diffraction Data Collected in Oscillation Mode. Methods in Enzymology", *Academic Press*, vol. 276, pp. 307-326, 1997